Heterogeneous Catalysis

Deutsche Ausgabe: DOI: 10.1002/ange.201700580
Internationale Ausgabe: DOI: 10.1002/anie.201700580

Spectroscopic Observation of a Hydrogenated CO Dimer Intermediate During CO Reduction on Cu(100) Electrodes

Elena Pérez-Gallent, Marta C. Figueiredo, Federico Calle-Vallejo, and Marc T. M. Koper**

Abstract: *Carbon dioxide and carbon monoxide can be electrochemically reduced to useful products such as ethylene and ethanol on copper electrocatalysts. The process is yet to be optimized and the exact mechanism and the corresponding reaction intermediates are under debate or unknown. In particular, it has been hypothesized that the C–C bond formation proceeds via CO dimerization and further hydrogenation. Although computational support for this hypothesis exists, direct experimental evidence has been elusive. In this work, we detect a hydrogenated dimer intermediate (OCCOH) using Fourier transform infrared spectroscopy at low overpotentials in LiOH solutions. Density functional theory calculations support our assignment of the observed vibrational bands. The formation of this intermediate is structure sensitive, as it is observed only during CO reduction on Cu(100) and not on Cu(111), in agreement with previous experimental and computational observations.*

A considerable number of experimental observations as well as density functional theory (DFT) calculations have established that CO_2 and CO reduction on copper electrodes forms C_1 and C_2 products through different reaction pathways.[1] The formation of C_1 and C_2 products has been shown to be highly sensitive to copper surface structure and electrolyte pH.[2] Hori et al.[2a] have shown that the CO to CH_4 reduction follows a concerted proton–electron transfer mechanism, in stark contrast with C_2H_4 production, the rate-limiting step of which is not sensitive to pH and only involves an electron transfer. As a result, on the pH-corrected RHE reference scale, the formation of ethylene from CO depends on pH while that of CH_4 does not.[2a,c] Furthermore, Schouten et al. have shown that C_2H_4 formation takes place preferentially at Cu(100) electrodes without simultaneous CH_4 formation, which indicates that the reaction paths towards CH_4 and C_2H_4 must bifurcate in the early stages of CO reduction.[2d] Specifically, a C_2 intermediate that requires only electron transfer, namely a negatively charged CO dimer, has been proposed as the first C–C coupled intermediate.[1a,2e,3] Various recent computational works have studied the structural sensitivity of this intermediate, and concluded that the formation of the dimer is indeed favored both thermodynamically and kinetically on Cu(100) sites compared to Cu(111).[3,4]

However, there is still no direct experimental evidence that proves CO dimerization in aqueous solution during CO reduction on copper electrodes, and the existence of the dimer is mostly a logical deduction from experimental and computational results. Here, we provide experimental evidence for the formation of a hydrogenated CO dimer (OCCOH) at low overpotentials during CO reduction on Cu(100) electrodes in LiOH solution, employing in situ Fourier transform infrared spectroscopy (FTIR), and support our interpretation by detailed DFT calculations.

Figure 1 shows the potential-dependent absorbance spectra of Cu(100) in 0.1 M LiOH solutions in Argon atmosphere

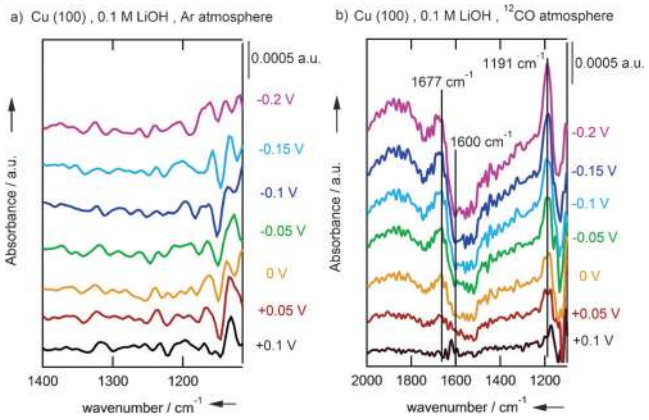

Figure 1. Potential-dependent absorbance spectra for Cu(100) in the a) absence and b) presence of CO in a 0.1 M LiOH solution. Reference spectrum recorded at +0.1 V vs. RHE. Highlighted bands and their corresponding frequencies are indicated with a vertical line at 1191 cm^{-1} for ^{12}C–OH stretching, 1677 cm^{-1} for ^{12}C=O stretching and 1600 cm^{-1} for O–H bending.

(Figure 1 a) and in CO atmosphere (Figure 1 b). The reference spectrum is taken at +0.1 V and additional spectra are provided for +0.05, 0.00, −0.05, −0.10, −0.15 and −0.2 V (all reported potentials are on the RHE scale). Full range FTIR spectra appear in the Supporting Information (SI), section S2. First of all, in Argon atmosphere the absorption spectra do not display any bands. After CO is bubbled through the solution, three bands appear at 1677, 1600 and 1191 cm^{-1}. The band at 1600 cm^{-1} corresponds to the O–H bending mode of H_2O. This band causes fluctuations in the baseline of the spectra making it difficult to identify other bands in this wavenumber range. The band at 1677 cm^{-1} corresponds to the C=O stretching[5] of CO adsorbed on hollow sites on Cu(100),

[*] E. Pérez-Gallent, Dr. M. C. Figueiredo, Dr. F. Calle-Vallejo, Prof. M. T. M. Koper
Leiden Institute of Chemistry, Leiden University
PO Box 9502, 2300 RA Leiden (The Netherlands)
E-mail: f.calle.vallejo@chem.leidenuniv.nl
m.koper@chem.leidenuniv.nl

Supporting information for this article can be found under: http://dx.doi.org/10.1002/anie.201700580.

in agreement with DFT calculations (see Figure 3 below). The intensity of the band for CO at multi bonded sites increases with more negative electrode potential. In alkaline media, the absolute potential (on the SHE scale) is more negative compared to acidic conditions and, consequently, the band for CO at multifold sites dominates the spectra.[6]

Simultaneously with the CO-related band, a band at 1191 cm^{-1} associated with C–OH stretching[7] grows in the spectra. Importantly, when CO reduction was performed under the exact same conditions on a Cu(111) electrode (see SI, Figure S1), the band at 1191 cm^{-1} and the band corresponding to C=O stretching at 1677 cm^{-1} were not observed. Figure 1a shows the absorbance spectra on Cu(100) without CO. The absence of the band at 1191 cm^{-1} strongly suggests that the signal appearing in CO atmosphere comes from a C-containing species. In order to ensure that the band at 1191 cm^{-1} comes from a C-containing species, a spectrum taken with isotopically labeled carbon ^{13}CO was recorded. When the absorbance spectra were obtained in ^{13}CO atmosphere (see Figure 2a), the band shifts from 1191 cm^{-1} to 1145 cm^{-1}. The shift of approximately 45 cm^{-1} matches the expected shift for the absorption spectra of ^{13}C compared to ^{12}C,[8] confirming that the band at 1191 cm^{-1} comes from a C-containing species.

As mentioned before, water exhibits a wide O–H bending band in the 1650–1450 cm^{-1} range, which prevents the straightforward observation of vibrations from other species in this wavenumber range. For this reason, CO reduction on Cu(100) was performed in D_2O; the corresponding spectra are shown in Figure 2b. In D_2O electrolyte, the range of 1650–1450 cm^{-1} is free of water bands, allowing for the identification of additional bands. Unfortunately, D_2O has an O–D bending band at 1209 cm^{-1} masking the C–OH stretching band. Interestingly, Figure 2b shows that in D_2O electrolyte at +0.05 V and more negative potentials a band appears around 1584 cm^{-1}, which corresponds to a C=O stretch but is not adsorbed CO.

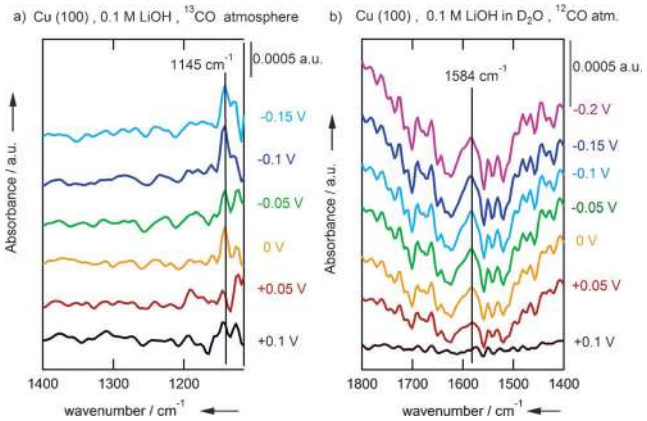

Figure 2. Potential dependent absorbance spectra for Cu(100) in the presence of a) ^{13}CO and with b) D_2O as electrolyte in a 0.1 M LiOH solution. Reference spectrum recorded at +0.1 V vs. RHE. Highlighted bands and their corresponding frequencies are indicated with a vertical line at 1145 cm^{-1} for ^{13}C–OH stretching and 1584 cm^{-1} for ^{12}C=O stretching.

From the combined results of the experiments in H_2O and D_2O, we observe two vibrational bands coming from C-containing species that are formed at low overpotentials on Cu(100) only. It is important to note that at the low overpotentials considered in our experiments, namely +0.1 to −0.15 V, no products are observed (for instance, the earliest onset potential on Cu(100) is that of C_2H_4 at −0.4 V).[2d,9] Thus, the bands in question should, in principle, be assigned to vibrations of adsorbed intermediates of CO reduction rather than to species in solution. To verify this hypothesis, we have scrutinized the IR spectra of various possible species in solution, including various C_1 and C_2 species.

Transmission spectra of species in solution such as formaldehyde, formate and methanol (C_1 molecules), and acetaldehyde and acetic acid (C_2 molecules) were recorded and are shown in Figure S2. The absence of the bands at 1191 and 1584 cm^{-1} in the transmission spectra rules out the possibility that the bands observed during the reduction of CO on Cu(100) correspond to these species in solution. Although methanol has a C–OH vibration at 1195 cm^{-1} in 0.1M LiOH, the vibration at 1584 cm^{-1} is absent (see SI, Figure S2c) and its substantially negative onset potential (−0.95 V[1d]) precludes the presence of methanol at the low overpotentials at which this work was performed (+0.1 to −0.15 V). The transmission spectra of acetaldehyde also displays a band at 1195 cm^{-1}, however, this band is associated with the C–OH stretching from the methanol present in the acetaldehyde solution as a stabilizer. In addition, acetaldehyde presents other two bands at 1712 and 1666 cm^{-1}. The absence of these bands in the spectra obtained during CO reduction rules out the possibility of acetaldehyde as a product. Another compound that could have vibrational frequencies close to those in Figure 1 and Figure 2 is acetylenediol (HOC≡COH). Maier et al. collected the infrared spectra of this double alcohol[10] and reported a single C–OH stretching band at 1212 cm^{-1}.

Having verified that the observed bands at 1191 and 1584 cm^{-1} do not correspond to species in solution, we now resort to DFT calculations to see whether a given adsorbed intermediate or a combination of them exhibit such bands. Since both CH_4 and C_2H_4 production from CO possess relatively early rate-limiting steps,[1c,11] we have limited our analysis to C_1 and C_2 species with no or a low content of hydrogen atoms (see Figure 3). First, consider the C_1 species CHO and COH (Figure 3b,c), which are the two possible products of the first hydrogenation of CO. They both have bands close to the band observed during the adsorption/reduction of ^{12}CO on Cu(100) at 1191 cm^{-1} (Figure 1b), but none of them exhibit the additional vibrational band at 1584 cm^{-1} (Figure 2b). Based on the experimental and DFT-calculated onset potential for CH_4 production on Cu(100) (≈ −0.8 V), and bearing in mind that CO protonation is deemed the potential-determining step of CO_2/CO reduction to CH_4,[12] we do not expect COH or CHO to be present at the low potentials at which our experiments were performed. The CO dimer (OCCO, Figure 3d) also presents a vibrational band at 1200 cm^{-1} but does not exhibit a band around 1584 cm^{-1}. Besides, a lithiated dimer (Figure 3e) features two

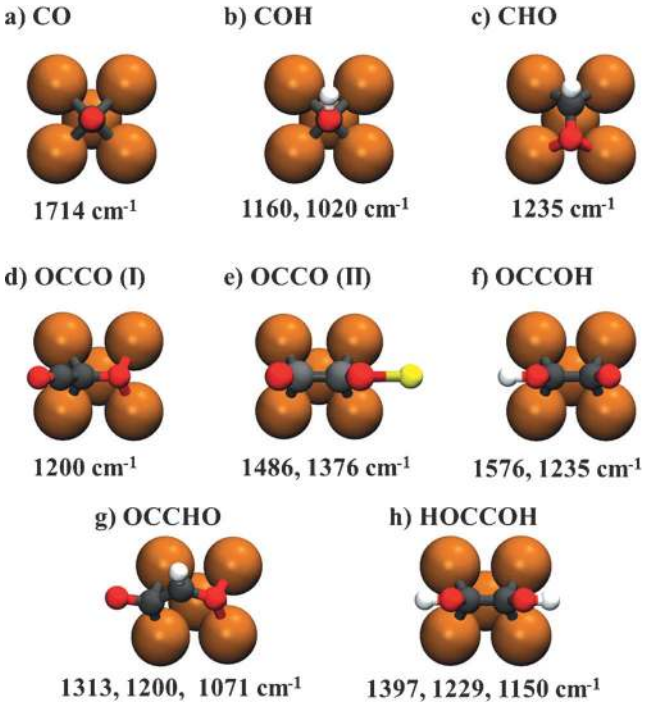

Figure 3. Schematic structures of possible adsorbed intermediates on Cu(100) and their calculated infrared-active vibrational frequencies in the 1100–1600 cm^{-1} wavenumber region. Cu, Li, C, O, and H atoms are depicted as orange, yellow, gray, red and white spheres.

C–O stretching frequencies that are not close to either of the bands at 1191 and 1584 cm^{-1}. Conversely, a CO dimer in which one of the oxygen atoms has been hydrogenated (OCCOH, Figure 3 f) exhibits bands close to both experimental bands. In addition, we have calculated the vibrational signatures of a CO dimer of which one of the carbon atoms has been hydrogenated (OCCHO, Figure 3 g). This adsorbate has vibrational bands around 1313, 1200, and 1071 cm^{-1} but no band close to 1584 cm^{-1}. Adsorbed acetylenediol, namely a doubly hydrogenated CO dimer (HOCCOH, Figure 3 h) was also considered in our DFT calculations. The predicted vibrational frequencies for C-OH stretching are 1397, 1229 and 1150 cm^{-1}. We also considered a simultaneously hydrogenated and lithiated dimer (HOCCOLi) and its vibrational frequencies were found at 1427 and 1246 cm^{-1}. Finally, a doubly lithiated dimer (LiOCCOLi) possesses C=O stretching frequencies at 1329 and 1261 cm^{-1}.

Therefore, we conclude that the bands at 1191 and 1584 cm^{-1} arise from C–O–H and C–O stretching vibrations and correspond, in the simplest case, to a hydrogenated dimer (OCCOH), or in general to this adsorbate in combination with other C_1 and C_2 adsorbates. This is in line with previous computational works showing that OCCOH is the most stable intermediate formed after the first hydrogenation of CO on Cu(100).[3]

In conclusion, we have shown experimentally that Cu(100) electrodes in LiOH solutions host a C-containing adsorbate at low overpotentials with vibrational bands at 1191 and 1584 cm^{-1}. Based on DFT calculations of a wide variety of C_1 and C_2 intermediates, we ascribe these bands to the C–O–H and C=O stretching modes of a hydrogenated CO dimer (OCCOH). These results provide for the first time direct confirmation of an important hypothesis in the electrocatalysis of CO_2 reduction on copper, namely that the C–C coupling to C_2 species on Cu(100) takes place through a reductive dimerization step at the early stages of the reaction mechanism. The fact that the vibrational features ascribed to the CO dimer could not be observed on Cu(111) under identical conditions confirms that CO dimerization is a structure-sensitive process favored by sites with square symmetry, in agreement with previous experimental[2f] and theoretical studies.[4b] We are currently performing further experiments and calculations to examine the influence of various alkaline cations on CO dimerization and their impact on the CO reduction pathway.

Experimental Section

Prior to each electrochemical experiment, the glassware used was stored overnight in a solution of $KMnO_4$ that was rinsed with a mixture of ultra clean water (Millipore MilliQ, resistivity $>18.2\,M\Omega$), $20\,mL\,L^{-1}$ of hydrogen peroxide and $1\,mL\,L^{-1}$ of concentrated sulfuric acid. The glassware was further cleaned by boiling 4 times in Millipore MilliQ water. A coiled platinum wire was used as counter electrode and a reversible hydrogen electrode (RHE) in the same electrolyte was used as reference electrode.

The copper electrodes used were 99.99% copper disks with a diameter of 6 mm, purchased from Mateck and aligned to $<0.5°$ accuracy. Prior to every experiment, the electrodes were electropolished and characterized as described elsewhere.[2b] Additional details appear in the SI, section S2.

The electrolytes were made from ultra-pure water (Millipore MilliQ, resistivity $>18.2\,M\Omega$) and high purity reagents (Sigma Aldrich TraceSelect). Before every experiment, Argon (Linde, 6.0) or CO (Linde 6.0) were bubbled through the electrolyte for 15 minutes in order to remove air from the solution or saturate the solution with CO, and during the experiments the corresponding gas was kept flowing above the solution.

FTIR measurements were performed with a Bruker Vertex 80 V Infrared spectrophotometer.[13] The electrochemical cell was assembled on top of a 60° CaF_2 prism, and the electrode was situated against this prism to form a thin layer. The measurements were performed under external reflection. FTIR spectra were obtained from an average of 100 scans with a resolution of $8\,cm^{-1}$ at the selected potentials. Every spectrum was obtained by applying single potential steps compared to the reference potential (+0.1 V). The spectra are shown as $(R-R_0)/R_0$ where R is the reflectance at the sample potential and R_0 is the reflectance at the reference potential. Thereby the ratio $\Delta R/R_0$ gives positive bands for the formation of species at the sample potential, while negative bands correspond to the loss of species at the sample potential. P-polarized light was used to probe species both near the electrode surface and in solution.

The vibrational frequencies were calculated by means of DFT calculations using the VASP code[14] with the PBE exchange-correlation functional[15] and the projector augmented wave (PAW) method.[16] The Cu(100) surfaces were modeled with (3×2) 4-layer-thick slabs. The vertical separation between periodically repeated images was more than 16 Å and dipole corrections were applied. The structures were optimized allowing the adsorbates and the two topmost layers to relax in all directions, while fixing the 2 bottom layers at the optimized bulk positions. The relaxations were carried out with a plane-wave cut-off of 450 eV, using the conjugate-gradient Scheme until the maximum force on any atom was below 0.05 $eV\,Å^{-1}$. The Brillouin zones were sampled with 6×8×1 Monkhorst-Pack meshes.[17] The Fermi level of the surfaces was smeared using the

Methfessel-Paxton method[18] with $k_B T = 0.2$ eV, and all energies were extrapolated to 0 K.

The vibrational frequency analysis was made using the harmonic oscillator approximation with two displacements in each direction plus the ground state.

Acknowledgements

F.C.V. acknowledges funding from the Netherlands Organization for Scientific Research (NWO), Veni project number 722.014.009. The use of supercomputing facilities at SURFsara was sponsored by NWO Physical Sciences, with financial support by NWO.

Conflict of interest

The authors declare no conflict of interest.

Keywords: CO dimer · CO reduction · DFT calculations · electrocatalysis · IR spectroscopy

How to cite: *Angew. Chem. Int. Ed.* **2017**, *56*, 3621 – 3624
Angew. Chem. **2017**, *129*, 3675 – 3678

[1] a) M. Gattrell, N. Gupta, A. Co, *J. Electroanal. Chem.* **2006**, *594*, 1 – 19; b) Y. Hori, I. Takahashi, O. Koga, N. Hoshi, *J. Phys. Chem. B* **2002**, *106*, 15 – 17; c) A. A. Peterson, F. Abild-Pedersen, F. Studt, J. Rossmeisl, J. K. Nørskov, *Energy Environ. Sci.* **2010**, *3*, 1311 – 1315; d) K. P. Kuhl, E. R. Cave, D. N. Abram, T. F. Jaramillo, *Energy Environ. Sci.* **2012**, *5*, 7050 – 7059; e) R. Kortlever, J. Shen, K. J. P. Schouten, F. Calle-Vallejo, M. T. M. Koper, *J. Phys. Chem. Lett.* **2015**, *6*, 4073 – 4082.

[2] a) Y. Hori, R. Takahashi, Y. Yoshinami, A. Murata, *J. Phys. Chem. B* **1997**, *101*, 7075 – 7081; b) K. J. P. Schouten, E. P. Gallent, M. T. M Koper, *J. Electroanal. Chem.* **2013**, *699*, 6 – 9; c) K. J. P. Schouten, E. P. Gallent, M. T. M. Koper, *J. Electroanal. Chem.* **2014**, *716*, 53 – 57; d) K. J. P. Schouten, Z. Qin, E. P. Gallent, M. T. M. Koper, *J. Am. Chem. Soc.* **2012**, *134*, 9864 – 9867; e) K. J. P. Schouten, Y. Kwon, C. J. M. Van der Ham, Z. Qin, M. T. M. Koper, *Chem. Sci.* **2011**, *2*, 1902 – 1909; f) K. J. P. Schouten, E. Pérez Gallent, M. T. M. Koper, *ACS Catal.* **2013**, *3*, 1292 – 1295; g) I. Ledezma-Yanez, E. Perez-Gallent, M. T. M. Koper, F. Calle-Vallejo, *Catal. Today* **2016**, *262*, 90 – 94.

[3] F. Calle-Vallejo, M. T. M. Koper, *Angew. Chem. Int. Ed.* **2013**, *52*, 7282 – 7285; *Angew. Chem.* **2013**, *125*, 7423 – 7426.

[4] a) J. H. Montoya, C. Shi, K. Chan, J. K. Nørskov, *J. Phys. Chem. Lett.* **2015**, *6*, 2032 – 2037; b) H. Li, Y. Li, M. T. M. Koper, F. Calle-Vallejo, *J. Am. Chem. Soc.* **2014**, *136*, 15694 – 15701.

[5] a) Y. Hori, O. Koga, Y. Watanabe, T. Matsuo, *Electrochim. Acta* **1998**, *44*, 1389 – 1395; b) R. Ryberg, *Surf. Sci.* **1982**, *114*, 627 – 641; c) M. Gajdoš, J. Hafner, *Surf. Sci.* **2005**, *590*, 117 – 126.

[6] a) S. C. Chang, M. J. Weaver, *J. Phys. Chem.* **1990**, *94*, 5095 – 5102; b) R. M. Arán-Ais, M. C. Figueiredo, F. J. Vidal-Iglesias, V. Climent, E. Herrero, J. M. Feliu, *Electrochim. Acta* **2011**, *58*, 184 – 192; c) S. K. Shaw, A. Berná, J. M. Feliu, R. J. Nichols, T. Jacob, D. J. Schiffrin, *Phys. Chem. Chem. Phys.* **2011**, *13*, 5242 – 5251; d) M. T. M. Koper, R. A. van Santen, *J. Electroanal. Chem.* **1999**, *476*, 64 – 70.

[7] G. Socrates, *Infrared and Raman Characteristic Group Frequencies: Tables and Charts*, Wiley, Hoboken, **2004**.

[8] M. W. Severson, C. Stuhlmann, I. Villegas, M. J. Weaver, *J. Chem. Phys.* **1995**, *103*, 9832 – 9843.

[9] F. Calle-Vallejo, J. Ignacio Martinez, J. Rossmeisl, *Phys. Chem. Chem. Phys.* **2011**, *13*, 15639 – 15643.

[10] G. Maier, C. Rohr, *Liebigs Ann.* **1996**, 307 – 309.

[11] a) F. Calle-Vallejo, J. I. Martínez, J. M. García-Lastra, E. Abad, M. T. M. Koper, *Surf. Sci.* **2013**, *607*, 47 – 53; b) X. Nie, M. R. Esopi, M. J. Janik, A. Asthagiri, *Angew. Chem. Int. Ed.* **2013**, *52*, 2459 – 2462; *Angew. Chem.* **2013**, *125*, 2519 – 2522.

[12] W. J. Durand, A. A. Peterson, F. Studt, F. Abild-Pedersen, J. K. Nørskov, *Surf. Sci.* **2011**, *605*, 1354 – 1359.

[13] G. García, P. Rodríguez, V. Rosca, M. T. M. Koper, *Langmuir* **2009**, *25*, 13661 – 13666.

[14] G. Kresse, J. Furthmüller, *Phys. Rev. B* **1996**, *54*, 11169 – 11186.

[15] J. P. Perdew, K. Burke, M. Ernzerhof, *Phys. Rev. Lett.* **1996**, *77*, 3865 – 3868.

[16] G. Kresse, D. Joubert, *Phys. Rev. B* **1999**, *59*, 1758 – 1775.

[17] H. J. Monkhorst, J. D. Pack, *Phys. Rev. B* **1976**, *13*, 5188 – 5192.

[18] M. Methfessel, A. T. Paxton, *Phys. Rev. B* **1989**, *40*, 3616 – 3621.

Manuscript received: January 17, 2017
Final Article published: February 23, 2017

